Why Does $SiLi_4$ Assume a Nontetrahedral (C_{2v}) Structure with Apparent Li-Li Attraction? Comparison with $GeLi_4$, $SnLi_4$, and CLi_4

Alan E. Reed,*,†,‡ Paul von Ragué Schleyer,† and Rudolf Janoschek§

Contribution from the Institut für Organische Chemie der Friedrich-Alexander-Universität Erlangen-Nürnberg, Henkestrasse 42, D-8520 Erlangen, Federal Republic of Germany, and Institut für Theoretische Chemie der Karl-Franzens-Universität Graz, Mozartgasse 14, A-8010 Graz, Austria. *Received November 20, 1989*

Abstract: The recently theoretically discovered nontetrahedral (C_{2v}) minimum energy structure of $SiLi_4$ violates both van't Hoff and electrostatic bonding principles. We supplement our previous work on $SiLi_4$ by considering the effect of electron correlation on the molecular geometry and by presenting a more detailed orbital analysis of the $SiLi_4$ wave functions. At the RHF level, it is shown that significant Li-Li bonding character arises through delocalization from the occupied Si-Li bonding orbitals into the 2s and 2p orbitals of the other Li atoms. MCSCF calculations on the C_{2v}, C_{3v}, and C_{4v} structures of $SiLi_4$ show only one excited configuration to be dominant, namely, that formed by the double excitation $...(A_1)^2 \rightarrow ...(A_1^*)^2$. The optimized MCSCF first excited A_1^* orbital exhibits pronounced Li_{eq}-Li_{eq} bonding. With respect to RHF, decreases of up to 0.2 Å in the "nonbonded" Li-Li distances in the C_{2v}, C_{3v}, and C_{4v} structures are found at the MCSCF, MP2, and CISD optimization levels, in accord with a significant correlation-induced increase in Li-Li bonding character. Similar results, but with longer Li-Li contacts, are found for $GeLi_4$ and $SnLi_4$. By contrast, the only ground-state minimum of CLi_4 is the T_d structure.

I. Introduction

That all potential bonding patterns of small molecules comprising only main group elements have not yet been discovered is shown by the recent theoretical discovery[1] that $SiLi_4$, though isoelectronic with SiH_4 and CLi_4,[2] is not tetrahedral but prefers a geometry of C_{2v} symmetry analogous to that of SF_4 (see Figure 1). A T_d structure for $SiLi_4$ would have been expected on the basis of both covalent and ionic bonding models.[3] On the other hand, one could regard $SiLi_4$ as a silicon atom interacting with an Li_4 cluster, in which case a symmetry less than T_d would be expected on the basis of extensive theoretical studies of Li clusters.[4] Two other low-energy structures for $SiLi_4$ were found[1] (Figure 1). The C_{4v} structure is a saddle point for interconversion between lithiums in axial and equatorial positions from the C_{2v} minimum-energy structure, and the C_{3v} structure is a double saddle point. Since all three structures of Figure 1 lie within about 3 kcal/mol, $SiLi_4$ is found to be a fluctional molecule, in further contrast to SiH_4.

Unusual structures that break conventional chemical bonding rules are typical for lithium compounds with elements such as carbon and silicon, especially when more than one lithium atom is present.[5,6] Though these structures may be less surprising from the viewpoint of the metallic cluster bonding models,[4] the C-Li and Si-Li bonding involved is quite ionic and these compounds can hardly be considered to be metallic alloys. Deviation from "normal" structures (with respect to traditional covalent bonding theory) is much more pronounced in lithiated silicon than in lithiated carbon compounds. Thus, although H_3CLi exhibits the expected "tetrahedral" structure of C_{3v} symmetry, there is a near energetic degeneracy between planar and "tetrahedral" (and singlet and triplet) forms of H_2CLi_2,[7] and, furthermore, H_3SiLi is found to prefer an inverted structure of C_{3v} symmetry of the form $Si(H_3)^-Li^+$ with ionic H-Li contacts.[8] Dilithiosilane, which prefers a tetrahedral structure of C_{2v} symmetry at the SCF level, is found to clearly prefer an inverted geometry of C_s symmetry when electron correlation energy is included.[9] This inverted structure can be roughly obtained from the tetrahedral C_{2v} structure by rotating one of the lithium atoms about silicon by 180° in the plane perpendicular to the H-Si-H plane; this "rotated" lithium atom engages in ionic bonding with the two H atoms. This bonding mechanism is of course not possible in $SiLi_4$, where, as discussed below, apparent Li-Li bonding occurs.

$SiLi_4$ has been synthesized by gas-phase reaction of Li atoms with $SiCl_4$,[10] but there has been no structural characterization of either the solid- or gas-phase material.[11] Numerous Zintl-Phase structures containing Si and Li have been synthesized, with stoichiometries of, for instance, Si_5Li_{21}, Si_4Li_{13}, and Si_7Li_{12} (and Ge_4Li_{14}, Ge_7Li_{12}).[12] The synthesis of an organodilithiosilane has been recently reported by Lagow and co-workers.[13]

To a first approximation, the bonding analysis of $SiLi_4$ is similar to that of SF_4, both species having a lone pair with high s character at the central atom and two 2-center-2-electron equatorial bonds. With regard to the axial substituents, $SiLi_4$ exhibits a 3-center-2-electron bond in place of the 3-center-4-electron bonding system

† Friedrich-Alexander-Universität Erlangen-Nürnberg.
‡ Present address: Bayer AG, AV-IM Angewandte Mathematik, 5090 Leverkusen, Federal Republic of Germany.
§ Karl-Franzens-Universität Graz.

(1) Schleyer, P. v. R.; Reed, A. E. *J. Am. Chem. Soc.* **1988**, *110*, 4453-4454.
(2) Würthwein, E.-U.; Sen, K. D.; Pople, J. A.; Schleyer, P. v. R. *Inorg. Chem.* **1983**, *22*, 496.
(3) An alternative electrostatic model involving Li^+ cations "bonded" at the surface of a perfectly spherical cloud of eight valence electrons on silicon yields a C_{4v} rather than a T_d structure if one allows the center of the sphere of the Si electrons to be displaced from the Si nucleus. Since the assumed spherically symmetric Si electron cloud is unrealistic, this model cannot be considered to provide an explanation for the nontetrahedral structure of $SiLi_4$. (Heilbronner, E., private communication; a somewhat analogous electrostatic model for the water molecule is presented in: Heilbronner, E. *J. Chem. Educ.* **1989**, *66*, 471-478.)
(4) (a) McAdon, M. H.; Goddard, W. A. *J. Phys. Chem.* **1987**, *91*, 2607-2626. (b) Koutecky, J. In Quantum Chemistry: Basic Aspects, Actual Trends. *Stud. Phys. Theor. Chem.* **1989**, *62*. (c) Messmer, R. P.; Tatar, R. C.; Briant, C. L. In *Alloying*; Walter, J. L., Jackson, M. R., Sims, C. T., Eds.; ASM International: Metals Park, OH, 1988; 29-88.
(5) Schleyer, P. v. R. *Pure Appl. Chem.* **1984**, *56*, 151.
(6) Setzer, W. N.; Schleyer, P. v. R. *Adv. Organomet. Chem.* **1985**, *23*, 353.
(7) Collins, J. B.; Dill, J. D.; Jemmis, E. D.; Apeloig, Y.; Schleyer, P. v. R.; Seeger, R.; Pople, J. A. *J. Am. Chem. Soc.* **1976**, *98*, 5419. Laidig, W. D.; Schaefer, H. F. *J. Am. Chem. Soc.* **1978**, *100*, 5972. Bachrach, S. W.; Streitwieser, A. *J. Am. Chem. Soc.* **1984**, *106*, 5818. Alvarado-Swaisgood, A. E.; Harrison, J. F. *J. Phys. Chem.* **1985**, *89*, 62. Sen, K. D.; Boehm, M. C.; Schmidt, P. C. *J. Mol. Struct. (THEOCHEM)* **1984**, *15*, 271.
(8) Schleyer, P. v. R.; Clark, T. *J. Chem. Soc., Chem. Commun.* **1986**, 1371.
(9) Rajca, A.; Wang, P.; Streitwieser, A.; Schleyer, P. v. R. *Inorg. Chem.* **1989**, *28*, 3064-3070.
(10) Morrison, J. A.; Lagow, R. J. *Inorg. Chem.* **1977**, *16*, 2972-2974.
(11) See also ref 8 of ref 1.
(12) (a) von Schnering, H. G.; Nesper, R.; Curda, J.; Tebbe, K.-F. *Angew. Chem.* **1980**, *92*, 1070; *Angew. Chem., Int. Ed. Engl.* **1980**, *19*, 1033. (b) Nesper, R. Lecture in Erlangen (Oct 25, 1988).
(13) Mehrotra, S. K.; Kawa, H.; Baran, J. R., Jr.; Ludvig, M. M.; Lagow, R. J. *J. Am. Chem. Soc.* **1990**, *112*, 9003-9004.

0002-7863/91/1513-1885$02.50/0

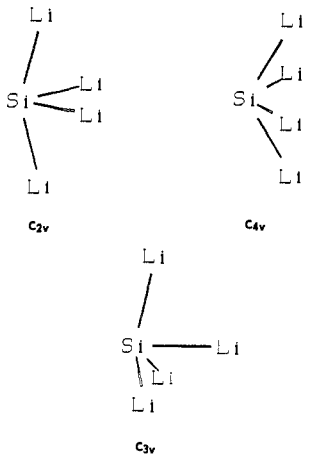

Figure 1. Plots of the MP2/3-21G(*) optimized structures for C_{2v} (left), C_{4v} (right), and C_{3v} (lower) $SiLi_4$.

of SF_4. The surprisingly small bond angles Li_{ax}–Si–Li_{ax} (162.3°), Li_{ax}–Si–Li_{eq} (83.5°), and Li_{eq}–Si–Li_{eq} (84.1°) suggested additionally the presence of attractive Li–Li bonding interactions in $SiLi_4$. Natural population analysis (NPA),[14] which revealed conclusively the ionic nature of tetrahedral CLi_4 (charge at each Li: +0.78),[15] shows C_{2v} $SiLi_4$ to have significant ionic character, with charges of +0.74 and +0.44 at the axial and equatorial lithium atoms.[1] The apparent attraction between the (strongly charged) lithium atoms is thus quite puzzling. We gave a brief explanation of how Li–Li attraction can arise through the delocalization of the occupied Si–Li bonding orbitals into virtual orbitals located mainly on other Li atoms,[1] as studied by natural bond orbital analysis (NBO).[14] This unusual feature of apparent Li–Li attraction is quite novel, and we therefore present the NBO analysis of $SiLi_4$ in this work in much greater detail than was possible in our initial paper.[1] Alternative analyses of the bonding in $SiLi_4$ have been presented by Bader[16] and by Epiotis.[17]

It is even more important, however, to study the possible influence of electron correlation on the structure of $SiLi_4$. Our previous $SiLi_4$ structures were obtained through calculations with the restricted Hartree–Fock method (RHF), involving single-determinant SCF wave functions. In addition, single-point energy calculations at the RHF geometries including electron correlation via Møller–Plesset perturbation theory to second order (MP2) were carried out. We noted, however,[18] that the RHF-SCF wave function for $SiLi_4$ is unstable upon removal of the spin restriction through the unrestricted HF (UHF) procedure. In other words, the SCF energy can be lowered by allowing the α and β spin SCF MOs to take on different spatial forms, resulting in spin polarization. It is of interest that both $SiLi_4$ and the Li_4 cluster exhibit UHF instability.[19] The electron correlation energy calculated from the RHF wave function (by the second-order RMP2 and fourth-order RMP4 methods) was found, however, to be very much greater than that calculated from the UHF wave function (by the UMP2 and UMP4 methods), and the RHF reference state led to a total energy (at MP2 or MP4) 10 kcal/mol lower than that of the UHF "state".[18] These results suggested that, although the RHF wave function is the best SCF starting point for calculations on $SiLi_4$ which include correlation energy, electron configurations other than the RHF-SCF ground configuration could be important.

An exploratory MCSCF study of $SiLi_4$ involving up to six configurations showed only one doubly excited configuration to be of dominant importance; this is of Si → Li_{eq} charge-transfer type. $SiLi_4$ thus exhibits diradical character analogous to that of singlet CH_2.[20] The MC-2 energy difference between the C_{2v} and C_{4v} structures changed little from the SCF value.[18] We therefore employ this simple MC-2 description further in our treatment of correlation in $SiLi_4$ and then compare it with the more elaborate MP2 and CISD treatments.

We also examine the related species $GeLi_4$ and $SnLi_4$ at the RHF level, to see if the preference for a C_{2v} geometry persists on going down the periodic table, and reexamine CLi_4.

The outline of our work is as follows. The theoretical methods employed are introduced under Section II. Under Section III, a detailed analysis of the RHF-SCF wave functions of $SiLi_4$ is given. Under Section IV, the effect of electron correlation and of basis set expansion and the possibility of a triplet state are treated. Under Section V, $GeLi_4$ and $SnLi_4$ are discussed. CLi_4 is reexamined under Section VI. Conclusions are given under Section VII.

II. Methods

Ab initio SCF calculations with the 3-21G(*) and 6-31G* basis sets[21] were carried out with the Gaussian 82 program.[22] For Ge and Sn, the split valence Huzinaga basis sets (43321/4321/4) and (433321/43321/43) were used, respectively, with the addition of a single d-orbital set for polarization.[23] Cartesian (6D) *d*-function sets were used for $SiLi_4$ and pure (5D) *d*-function sets for $GeLi_4$ and $SnLi_4$. The MOLEKEL[24] program was applied to the previous exploratory MCSCF calculations, and the GAMESS[25] program was employed for the MCSCF[26] geometry optimizations with analytic gradients. Geometry optimizations including electron correlation via second-order Møller–Plesset perturbation theory or via configuration interaction with single and double substitutions (CISD), in both cases employing analytic gradients, were carried out with the Gaussian 82 and Gaussian 86 programs.[21,22] Generalized valence bond (GVB)[27] calculations were done with the GAMESS and Gaussian 86 programs.

The calculated wave functions were analyzed with the G82NBO program.[14e] A recent paper summarizes the NBO method and its previous application.[14f] The first step is to carry out natural population analysis (NPA); natural populations are the occupancies of the orthogonal natural atomic orbitals (NAOs).[14b] Natural bond orbitals (NBOs)[14a] are then computed in the NAO basis, these are the localized 1- and 2-center orbitals that form an orthogonal set. The NBOs correspond to molecular Lewis structures. The NBO Lewis structure is then allowed to delocalize so that all core, lone pair, and bond orbitals become doubly occupied,

(14) (a) Foster, J. P.; Weinhold, F. *J. Am. Chem. Soc.* **1980**, *102*, 7211. (b) Reed, A. E.; Weinstock, R.B.; Weinhold, F. *J. Chem. Phys.* **1985**, *83*, 735–746. (c) Reed, A. E.; Weinhold, F. *J. Chem. Phys.* **1985**, *83*, 1736–1740. (d) Reed, A. E. Ph.D. Dissertation, University of Wisconsin—Madison, 1985; *Diss. Abstr. Int.* **1986**, *46*, 4259B. (e) Reed, A. E.; Weinhold, F. *QCPE* **1985**, *5*, 141–142. (f) Reed, A. E.; Weinhold, F.; Curtiss, L. A. *Chem. Rev.* **1988**, *88*, 899–926.

(15) Reed, A. E.; Weinhold, F. *J. Am. Chem. Soc.* **1985**, *107*, 1919–1921.

(16) Bader, R. W. F. Private communication. On the basis of Bader's electron density analysis, Li–Li bonding is *not* involved.

(17) Epiotis, N. D. *New J. Chem.* **1989**, *13*, 829–833. Epiotis presents a qualitative discussion of the bonding without quantitative calculation.

(18) See ref 9 in ref 1.

(19) McAdon, M. H.; Goddard, W. A. *J. Chem. Phys.* **1988**, *88*, 277. McAdon, M. H.; Goddard, W. A. *J. Phys. Chem.* **1988**, *92*, 1352–1365.

(20) (a) Bauschlicher, C. W.; Schaefer, H. F.; Bagus, P. S. *J. Am. Chem. Soc.* **1977**, *99*, 7106. (b) Goddard, W. A. *Science* **1985**, *227*, 917–923. (c) Hay, P. J.; Hunt, W. J.; Goddard, W. A. *J. Am. Chem. Soc.* **1972**, *94*, 8293–8301.

(21) Hehre, W. J.; Radom, L.; Schleyer, P. v. R.; Pople, J. A. *Ab Initio Molecular Orbital Theory*; Wiley: New York, 1986.

(22) (a) Binkley, J. S.; Frisch, M. J.; DeFrees, D. J.; Raghavachari, K.; Whiteside, R. A.; Schlegel, H. B.; Fluder, E. M.; Pople, J. A. *Gaussian 82* (release H version); Carnegie-Mellon University: Pittsburgh, PA, 1983. This program was modified by Convex for the Convex C-1. (b) Hehre, W. J.; Radom, L.; Schleyer, P. v. R.; Pople, J. A. *Ab Initio Molecular Orbital Theory*; Wiley: New York, 1986. (c) Frisch, M. J.; Binkley, J. S.; Schlegel, H. B.; Raghavachari, K.; Melius, C. F.; Martin, R. L.; Stewart, J. J. P.; Bobrowicz, F. W.; Rohlfing, C. M.; Kahn, L. R.; DeFrees, D. J.; Seeger, R.; Whiteside, R. A.; Fox, D. J.; Fluder, E. M.; Pople, J. A. *Gaussian 86*; Carnegie-Mellon Quantum Chemistry Publishing Unit: Pittsburgh, PA, 1984.

(23) Huzinaga, S.; Andzelm, J.; Klobukowski, M.; Radzio-Andzelm, E.; Sakai, Y.; Tazewaki, H. *Gaussian Basis Sets for Molecular Calculations*; Elsevier: New York, 1984.

(24) Werner, H. J.; Meyer, W. *J. Chem. Phys.* **1981**, *74*, 5794. Werner, H. J.; Reinsch, E. A. *J. Chem. Phys.* **1982**, *76*, 3144.

(25) Schmidt, M. W.; Boatz, J. A.; Baldridge, K. K.; Koseki, S.; Gordon, M. S.; Elbert, S. T.; Lam, D. GAMESS Program, QCPE Newsletter, Fall 1987. Original version: Dupuis, M.; Spangler, D.; Wendoloski, J. J. National Resource for Computations in Chemistry, Software Catalog, Vol. 1, Program QG01, 1980, Lawrence Berkeley Laboratory, USDOE. The program was adapted to the Convex C-120 by Dr. J. Kaneti.

(26) Yaffe, L. G.; Goddard, W. A. *Phys. Rev. A* **1976**, *13*, 1682.

(27) (a) Bobrowicz, F. W.; Goddard, W. A. In *Modern Theoretical Chemistry*; Schaefer, H. F., III, Ed.; Plenum: New York, 1977; Vol. 3, Chapter 4. (b) Goddard, W. A.; Dunning, T. H.; Hunt, W. J.; Hay, P. J. *Acc. Chem. Res.* **1973**, *6*, 368–376. (c) Reference 20c.

forming the natural localized molecular orbitals (NLMOs).[14c] The NLMOs are similar in form to localized molecular orbitals derived by other methods.[14d]

Orbital contour plots were performed with the ORBCONT program.[28] Since the NBOs form an orthogonal set, and, thus, donor and acceptor NBOs have zero overlap, the nonorthogonal NBOs (NONBOs) are employed for judging donor–acceptor overlap.[14f,29] The NONBOs are formed from the NBOs by omitting the interatomic orthogonalization step, as described previously,[29] and lack the orthogonalization tails of the NBOs. Thus, instead of plotting NBOs, we plot the corresponding NONBOs.

Calculations were carried out on Convex C-120 and C-210 computers at Erlangen and on a VAX 3200 computer at the Rechenzentrum der Universität Graz.

III. Analysis of RHF/3-21G(*) Wave Functions for $SiLi_4$

A. NBO Lewis Structure. The NBO method seeks to represent the electronic structure of a molecule in terms of the best possible resonance Lewis structure consisting of core, lone pair, and strictly localized (2-center, and if necessary, 3-center) bond orbitals. This set of high-occupancy natural bond orbitals (NBOs) is then augmented by the corresponding antibonds and by single-center, extra-valence-shell orbitals (designated Rydberg NBOs). For the C_{2v} structure of $SiLi_4$, application of the NBO program, allowing search for 3-center bonds, results in the following Lewis structure: Two $\sigma(Si–Li_{eq})$ bonds, one $Li_{ax}–Si–Li_{ax}$ 3-center–2-electron bond, and one lone pair on Si (n_{Si}). The $\sigma(Si–Li_{eq})$ bonds are polarized 73% toward Si and are composed from hybrids of 96% p character on Si and 98% s character on Li and have occupancies of 1.86 e. The 3c bond is more ionic, 83% polarized toward Si, with nearly pure p character on Si (99.9%) and 95% s character on the two lithiums, and has an occupancy of 1.95 e. The n_{Si} orbital is 93% s and 7% p and has an occupancy of 1.92 e. Note that n_{Si} is basically pure Si 3s and that the Si–Li bonds involve nearly pure Si 3p character. This is in line with the general tendency of second-row atoms to form bonds with high p character and lone pairs with high s character.[30] The axial bonds are significantly shorter than the equatorial bonds (2.43 vs 2.51 Å), in line with their greatly increased ionic character.

Is it at all possible to represent the wave function for the C_{2v} structure of $SiLi_4$ with an NBO Lewis structure having four Si–Li bonds and without a lone pair on Si? It is possible override the automatic NBO search procedure and to force the NBO program to attempt to form a particular Lewis structure of bonds and lone pairs. When the formation of zero Si lone pairs and four Si–Li 2-center bond NBOs is forced, one of these is found to be polarized 99% toward Si and has over 90% s character and is very similar to the n_{Si} lone pair formed by the standard NBO search procedure. It is thus impossible to form four true Si–Li bonds because of high-occupancy lone pair on Si in the C_{2v} structure. If one bends the $Li_{ax}–Si–Li_{ax}$ angle strongly *outward* so that the geometry becomes closer and closer to being tetrahedral, the NBO analysis reveals that n_{Si} gradually loses both in occupancy and in s character. When the axial lithiums are bent far enough toward the T_d structure, the influence of valence 3s–3p hybridization at Si becomes strong enough that an NBO Lewis structure with a lone pair on Si is unfavorable and four Si–Li bonds are formed, just as for the T_d structure.

B. NBO Donor–Acceptor Interactions. Delocalization from the above localized NBO Lewis structure in C_{2v} $SiLi_4$ is quite significant, however, as the occupancies of the formally fully occupied orbitals deviate significantly from 2.00. Indeed, a total of 0.42 e is delocalized into acceptor orbitals. The major acceptor orbitals are the $\sigma^*(Si–Li_{eq})$ antibonds (73% polarized toward Li, with 96% s character), the Li 2p orbitals, and the formally unoccupied orbitals associated with the 3c bond. Now, just as each 2-center bond orbital has a 2-center antibond associated with it, a 3c bond orbital has in general an associated 3c nonbond and a 3c antibond orbital. Normally, the 3c bond, nonbond, and antibond orbitals have 0, 1, and 2 nodes perpendicular to the bond axis. Due to the dominant contribution from the axial Si 3p orbital, the 3c bond in C_{2v} $SiLi_4$ has one node, with the consequence that the formally empty 3c "nonbonding" orbital is nodeless; it has in-phase bonding contributions from the Li_{ax} atoms and no contribution from the Si atom (such a contribution is ruled out by symmetry, since the Si atom contributes a π-type hybrid to the 3c bond). We therefore prefer to denote this nodeless 3c nonbond orbital the 3c acceptor orbital. The last orbital, the 3c antibond, has mainly contributions from Li 2s orbitals with a smaller, antibonding contribution from the Si axial 3p orbital and thus has three nodes. The relative importance of these acceptor orbitals is reflected by their occupancies: 0.021 e for $\sigma^*(Si–Li_{eq})$, 0.12 e for the 3c acceptor, 0.0008 e for the 3c antibond, and a total of 0.29 e for the Li 2p orbitals (0.083 e on each Li_{eq} and 0.061 e on each Li_{ax}).

Thus, more than half of the 0.42 e delocalization goes into Li 2p orbitals. The importance of the Li 2p delocalization is evident when the Li 2p orbitals are removed from the basis set: geometry optimization of the C_{2v} structure leads to the T_d structure, which is now the energy minimum. In the absence of Li 2p orbitals, no C_{2v} minimum exists for $SiLi_4$.

The second-order perturbational analysis of the NBO Fock matrix printed by the NBO program shows at a glance which interactions are more important. On the basis of the second-order stabilization energies $E^{(2)}$, the most prominent delocalizations are (1) $\sigma(Si–Li_{eq}) \rightarrow$ 3c acceptor (two identical interactions, each 21 kcal/mol) and (2) $n_{Si} \rightarrow$ 3c acceptor (31 kcal/mol). Individually, the interactions with the Li 2p orbitals are much weaker, but these are numerous and the $E^{(2)}$ values total to 40 kcal/mol. These include the following: (3) 3c bond $\rightarrow Li_{eq}(2p)$, involving $Si(3p_\pi) \rightarrow Li_{eq}(2p_\pi)$ π bonding (two such interactions, each 7 kcal/mol); (4) $\sigma(Si–Li_{eq,A}) \rightarrow Li_{eq,B}(2p)$, involving $Si(3p) \rightarrow Li(2p)$ π bonding *within* the $Li_{eq}–Si–Li_{eq}$ plane (two such interactions, each 6 kcal/mol); (5) $\sigma(Si–Li_{eq}) \rightarrow Li_{ax}(2p)$, involving $Si(3p) \rightarrow Li(2p)$ π bonding *within* $Li_{eq}–Si–Li_{ax}$ plane (four such interactions, each 3 kcal/mol); (6) $n_{Si} \rightarrow Li_{ax}(2p)$, involving donation from Si(3s) into the $Li_{ax}(2p)$ orbital directed along the axial bond axis (two such interactions, each 2 kcal/mol).

There are two ways of illustrating these delocalization interactions, first, by the donor–acceptor (NONBO) overlap and, second, through the forms of the natural localized molecular orbitals (NLMOs). The NLMOs have occupancies of either exactly two or zero (RHF level) and are formed by allowing each *strictly localized* NBO Lewis structure orbital to delocalize as little as possible to make it doubly occupied. Parts a and c of Figure 2 show the overlap of the $\sigma(Si–Li_{eq})$ NONBO with the 3c acceptor and $Li_{eq}(2p)$ NONBOs, respectively [the overlap with $Li_{ax}(2p)$ is similar]. Parts b and d of Figure 2 show the $\sigma(Si–Li_{eq})$ NLMO in the $Li_{ax}–Si–Li_{eq}$ and $Li_{eq}–Si–Li_{eq}$ planes, respectively; note how the $\sigma(Si–Li_{eq})$ orbital has been "stretched" in the direction of the second lithium atom in the respective planes in comparison with the form of the $\sigma(Si–Li_{eq})$ NONBO in Figure 2a,c. A significant Li–Li bonding interaction is evident from these figures. Parts a and b of Figure 3 show respectively the 3c bond $\rightarrow Li_{eq}(2p)$ NONBO overlap and the 3c bond NLMO, illustrating the resulting $\pi(Si–Li_{eq})$ and $\sigma(Li_{ax}–Li_{eq})$ bonding interactions. Parts a and b of Figure 4 show respectively the $n_{Si} \rightarrow$ 3c acceptor NONBO overlap and the n_{Si} NLMO, depicting the stretching of n_{Si} toward the Li_{ax} atoms and the resulting increased $Si–Li_{ax}$ covalent bonding. Clearly, the $n_{Si} \rightarrow$ 3c acceptor interaction will favor an *outward* bending of the $Li_{ax}–Si–Li_{ax}$ angle. This, however, is the only interaction that favors an increased $Li_{ax}–Si–Li_{ax}$ angle, and the centroid of the n_{Si} orbital does not lie far enough from Si to make this influence on the angle dominant.

C. Relation to MO Description. It is of interest to note the relationship of the occupied valence NLMOs to the canonical MOs. The energies (au) and symmetries of the valence shell MOs are −0.49 (A_1), −0.21 (B_1), −0.177 (B_2), and −0.171 (A_1). The B_1 MO corresponds to the $Li_{ax}–Si–Li_{ax}$ 3c bond NLMO and the

(28) The orbital contour diagrams were made by using the ORBCONT program supplied by Dr. J. Carpenter and Dr. E. Glendening, University of Wisconsin—Madison.

(29) Reed, A. E.; Schleyer, P. v. R. *J. Am. Chem. Soc.* **1987**, *109*, 7362–7371.

(30) Kutzelnigg, W. *Angew. Chem.* **1984**, *96*, 262; *Angew. Chem., Int. Ed. Engl.* **1984**, *23*, 272, and references cited therein.

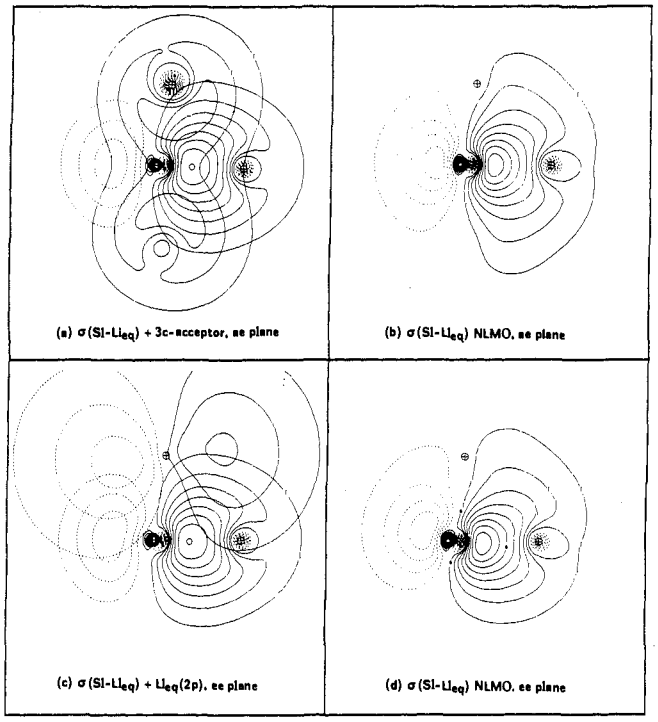

Figure 2. Orbital contour plots (10 contours, lowest contour 0.016 au) from C_{2v} $SiLi_4$, RHF/3-21G(*) calculation, showing overlap of the σ-(Si–Li_{eq}) NONBO with (a) the 3c acceptor NONBO in the Li_{ax}–Si–Li_{eq} plane and with (c) the Li_{eq}(2p) NONBO in the Li_{eq}–Si–Li_{eq} plane. The effect of these delocalizations is seen in the form of the σ(Si–Li_{eq}) NLMO, depicted in the Li_{ax}–Si–Li_{eq} (b) and Li_{eq}–Si–Li_{eq} (d) planes.

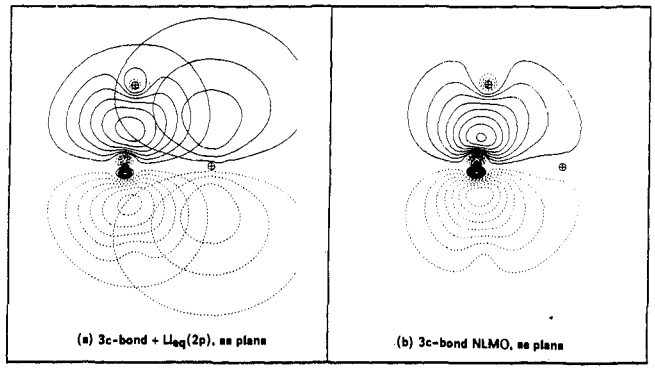

Figure 3. As Figure 2, and showing, in the Li_{ax}–Si–Li_{eq} plane, (a) the 3c bond–Li_{eq}(2p) NONBO overlap and (b) the 3c bond NLMO.

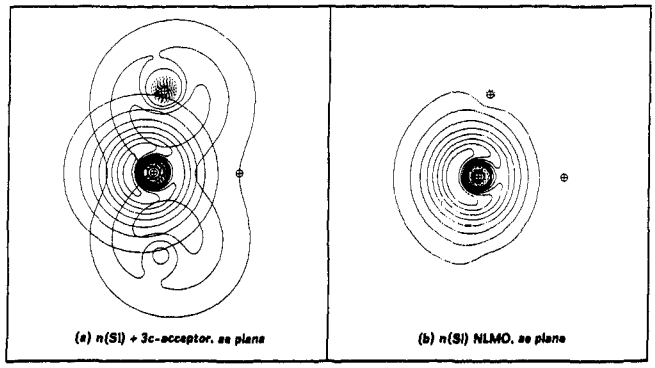

Figure 4. As Figure 2, and showing, in the Li_{ax}–Si–Li_{eq} plane, (a) the n_{Si}–3c acceptor NONBO overlap and (b) the n_{Si} NLMO.

B_2 MO to the antisymmetric combination of the two σ(Si–Li_{eq}) NLMOs. The symmetric combination of the two σ(Si–Li_{eq}) NLMOs mixes somewhat with the n_{Si} NLMO in the formation of the two A_1 valence MOs, the lower energy A_1 MO consisting mainly of the n_{Si} NLMO and the higher energy A_1 MO (the HOMO) consisting mainly of the symmetric combination of the two σ(Si–Li_{eq}) NLMOs, and a much smaller *antibonding* contribution from n_{Si}. Since only the symmetric combination of the two σ(Si–Li_{eq}) NBOs can delocalize into the 3c acceptor NBO, the σ(Si–Li_{eq}) → 3c acceptor interaction occurs solely in the HOMO. The other interactions contributing to Li–Li covalent bonding, donation from σ(Si–Li_{eq}) and the 3c bond into Li 2p orbitals, are spread among the B_1, B_2, and A_1 (HOMO) MOs. The significant covalent Li–Li bonding interactions within the HOMO are evident from Figure 5a,c. The HOMO has a maximum along the bisector of the Li_{eq}–Si–Li_{eq} angle, emphasizing the Li_{eq}–Li_{eq} bonding character.

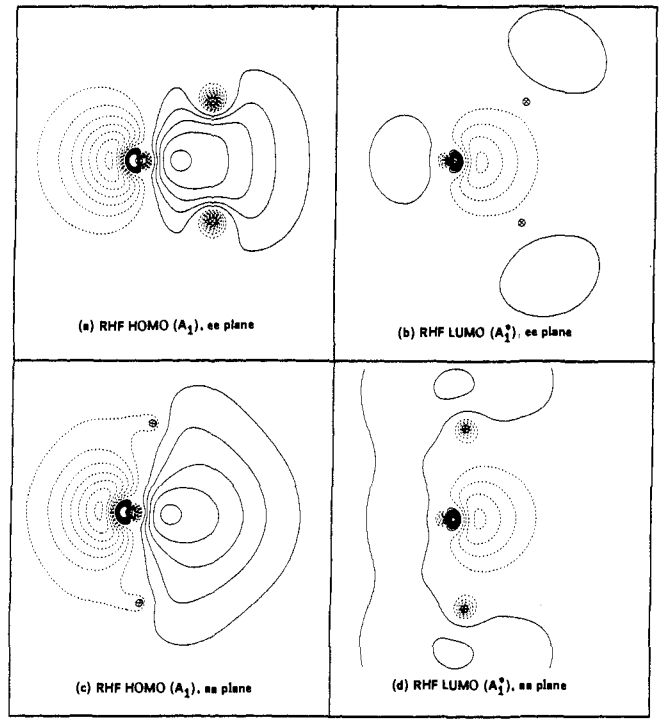

Figure 5. As Figure 2, and showing the RHF HOMO and LUMO in the Li_{eq}–Si–Li_{eq} and Li_{ax}–Si–Li_{ax} planes.

D. Summary. The above NBO description of C_{2v} $SiLi_4$ demonstrates that covalent Li–Li bonding comes about through the delocalization of Si–Li bonding orbitals [σ(Si–Li_{eq}) and the 3c bond] into formally empty orbitals (3c nonbond, Li 2p) that have primary contributions from Li 2s and 2p orbitals. $SiLi_4$ is rather ionic, with charges by NPA at Li_{ax} and Li_{eq} of +0.74 and +0.44, respectively. In the absence of this significant ionic character, Li–Li covalent bonding interactions in $SiLi_4$ would be much weaker, since the Li valence orbitals would have higher occupancy and energy (as do the H orbitals in SiH_4). At the RHF level of theory, there are thus three important factors which *together* are responsible for the favored C_{2v} structure of $SiLi_4$: (a) the significant ionicity of the Si–Li bond, which opens up the possibility of a $SiLi_4$ structure involving a lone pair on Si; (b) the tendency of second-row atoms such as Si to concentrate s character in lone pair hybrids and p character in bonding hybrids,[30] opening up the possibility of a $SiLi_4$ structure where Si first forms two 2-center bonds with Li atoms employing two of the Si 3p orbitals (hence, a ca. 90° Li_{eq}–Si–Li_{eq} angle) and second a linear 3-center bond with the remaining two Li atoms employing the remaining Si 3p orbital (hence, a ca. 180° Li_{ax}–Si–Li_{ax} angle and ca. 90° Li_{ax}–Si–Li_{eq} angles); (c) covalent Li–Li bonding through σ(Si–Li_{eq}), 3c bond → 3c nonbond, Li 2p delocalization, enabling Li_{ax}–Si–Li_{eq} and Li_{eq}–Si–Li_{eq} angles of less than 90°. All three of these factors are important. In CLi_4 factor b is missing, and a tetrahedral structure is preferred (it may also be that the Li–Li distances in a hypothetical C_{2v} structure of CLi_4 would be too short to be able to overcome the electrostatic repulsion, and the fact that the lithiums have larger positive charges in CLi_4 than in $SiLi_4$ may also be important). In SiH_4, factors a and c are missing. That

Table I. Optimized Geometries and Energies of $SiLi_4$ Isomers[a]

sym	method	energy[b]	SiA	SiE	AE	EE	ASiA	ASiE	ESiE
			3-2sp1sG(Li)/3-21G(Si)[c] Basis Set						
C_{2v}	RHF	−316.983 29 (0.00)	2.419	2.534	3.352	3.324	167.1	85.1	82.0
	MC-2	−316.999 98 (0.00)	2.437	2.546	3.308	3.121	162.6	83.2	75.6
C_{3v}	RHF	−316.981 79 (0.94)	2.555	2.444	3.317	4.202		83.1	118.6
	MC-2	−316.998 00 (1.24)	2.617	2.477	3.235	4.209		78.8	116.3
C_{4v}	RHF	−316.974 36 (5.60)	2.548	2.548	3.123	4.416	120.2	75.6	120.2
	MC-2	−316.989 54 (6.55)	2.556	2.556	3.086	4.365	117.3	74.3	117.3
T_d	RHF	−316.980 26 (1.90)	2.420		3.953				
			3-21G(*) Basis Set						
C_{2v}	RHF	−317.041 46 (0.00)	2.429	2.514	3.291	3.368	162.3	83.5	84.1
	MC-2	−317.058 64 (0.00)	2.444	2.525	3.256	3.227	158.8	81.9	79.4
	MP2	−317.196 14 (0.00)	2.451	2.505	3.166	3.218	152.2	79.4	79.9
	CISD	−317.192 15 (0.00)	2.440	2.507	3.166	3.230	152.6	79.6	80.2
C_{3v}	RHF	−317.038 15 (2.08)	2.527	2.442	3.332	4.208		84.2	119.0
	MC-2	−317.053 09 (3.48)	2.574	2.481	3.187	4.206		78.1	115.9
	MP2	−317.191 97 (2.62)	2.510	2.461	3.096	4.154		77.0	115.1
	CISD	−317.187 90 (2.67)	2.526	2.454	3.108	4.144		77.2	115.3
C_{4v}	RHF	−317.035 54 (3.71)	2.505	2.505	3.151	4.456	125.6	77.9	125.6
	MC-2	−317.052 44 (3.89)	2.523	2.523	3.114	4.404	121.6	75.9	121.6
	MP2	−317.190 69 (3.42)	2.508	2.508	3.097	4.379	121.6	76.2	121.6
T_d	RHF	−317.035 55 (3.71)	2.420		3.953				
	MP2	−317.184 57 (7.26)	2.411		3.937				
			6-31G* Basis Set						
C_{2v}	RHF	−318.670 98 (0.00)	2.408	2.499	3.274	3.360	162.9	83.7	84.5
	MC-2	−318.687 63 (0.00)	2.426	2.509	3.235	3.208	158.9	81.9	79.5
	MP2	−318.845 02 (0.00)	2.396	2.459	3.198	3.246	159.7	82.4	82.6
C_{3v}	RHF	−318.668 21 (1.74)	2.515	2.422	3.249	4.157		82.3	118.2
	MP2	−318.840 41 (2.89)	2.476	2.417	3.077	4.093		77.9	115.7
C_{4v}	RHF	−318.666 06 (3.09)	2.485	2.485	3.139	4.439	126.6	78.3	126.6
	MP2	−318.838 68 (3.98)	2.473	2.473	3.082	4.336	122.4	76.6	122.4
T_d	RHF	−318.665 42 (3.49)	2.395		3.911				
	MP2	−318.833 84 (7.02)	2.367		3.865				

[a] In the bond length and angle designations, the axial and equatorial lithium atoms are designated A and E, respectively. Distances in Å, angles in deg. [b] Total energy in au, and, in parentheses, relative energy in kcal/mol. [c] In the 3-2sp1sG(Li) basis set, the outer lithium 2p orbitals have been omitted from the 3-21G basis (in this notation, the full 3-21G basis set for Li would be 3-2sp1sp).

factor b is quite important in silicon compounds is illustrated by the structure of Si_2H_2, which is doubly bridged with the two Si–H–Si planes being nearly perpendicular to each other[31] and involves a lone pair of high s character on each silicon and Si–Si and Si–H bonds of high Si p character.[32]

IV. Higher Level Calculations on $SiLi_4$

A. Influence of Electron Correlation. Our previous, exploratory MCSCF calculations at fixed geometries showed, besides the main configuration, a single $(A_1)^2 \rightarrow (A_1^*)^2$ configuration to dominate over the others in C_{2v} and C_{4v} $SiLi_4$. For the purpose of initial exploratory geometry optimizations, we started with a much smaller basis set for $SiLi_4$ than 3-21G(*) by removing the d orbitals of Si (3-21G basis for Si) and the outer set of p orbitals of Li (the "1" set of p orbitals in the 3-21G basis). This basis set can be designated 3-2sp1sG(Li)/3-21G(Si), and we call it basis set A. The number of basis functions is then reduced from 55 to 37. This basis set gives RHF geometries for the various $SiLi_4$ structures that are similar to those of the 3-21G(*) basis set, as seen from Table I. In the C_{2v} structure, for instance, the Li_{ax}–Li_{eq} distance is 0.06 Å longer as compared with 3-21G(*) [probably due to weaker $\sigma(Si–Li_{eq}) \rightarrow Li_{ax}(2p)$ donation] and the Li_{eq}–Li_{eq} distance is 0.04 Å shorter (probably due to the weaker Li_{eq}–Li_{ax} bonding). Table I shows the results of our MC-2 geometry optimizations with basis set A. For each of the C_{2v}, C_{3v}, and C_{4v} structures, the second configuration involved an $(A_1)^2 \rightarrow (A_1^*)^2$ excitation. In the T_d structure, however, such an excitation was found to be of little importance, and the most important excited configurations are triply degenerate. MCSCF calculations with a larger number of configurations would therefore have to be performed to be able to compare the T_d structure with the other structures on a more or less balanced basis. The relative energies of the C_{2v}, C_{4v}, and C_{3v} structures are basically unchanged from the RHF to the MC-2 levels. Significant decreases in Li–Li distances of up to 0.2 Å occur, however, showing that inclusion of the second configuration increases the Li–Li bonding interaction.

We then repeated these MC-2 calculations with the full 3-21G(*) basis set. As seen from Table I, the changes in energies and geometries on going from RHF to MC-2 are similar with basis A and with 3-21G(*), the maximum decrease in a Li–Li distance with 3-21G(*) on going to MC-2 being smaller at 0.14 Å.

The square of the coefficient of the second configuration in each MC-2 wave function is around 0.08; that is, the excited configuration contributes 8% to the wave function, compared to a contribution of 4% from the excited configuration of singlet CH_2 to its MC-2 wave function.[20] By NPA, the axial lithiums in the C_{2v} structure have the same charge as at the RHF level, and there is a transfer of 0.11 e from Si to the equatorial lithiums. In line with this, the molecular dipole moment decreases from 3.65 to 2.46 D from SCF to MC-2. In the C_{3v} structure, the charge on the equatorial lithiums is unchanged on going to MC-2; 0.20 e is transferred from Si to the axial lithium, and the dipole moment decreases from 2.10 to 0.59 D. In the C_{4v} structure, Si loses 0.06 e to the four lithium atoms at MC-2, and the dipole moment decreases moderately from 2.73 to 2.66 D.

Interestingly, the second (excited configuration) orbital of the converged MC-2 calculation on the C_{2v} structure is rather different in form from the LUMO derived from the RHF calculation. The RHF LUMO is quite diffuse (Figure 5b,d), in vivid contrast to the relatively compact MC-2 excited orbital (Figure 6b,d). The first (ground configuration) MC-2 orbital is quite similar to the RHF HOMO but is slightly more polarized toward silicon, as seen by comparing Figure 5a,c with Figure 6a,c. Indeed, the first and second MC-2 orbitals in Figure 6 are quite similar in their form, the second (excited) orbital being significantly more polarized toward the Li_{eq} atoms and having an extra node to maintain

(31) Luke, B. T.; Pople, J. A.; Krogh-Jespersen, M.-B.; Apeloig, Y.; Karni, M.; Chandrasekhar, J.; Schleyer, P. v. R. *J. Am. Chem. Soc.* **1986**, *108*, 270–284, and ref 81–83 therein.

(32) Analysis: Reed, A. E. Unpublished results.

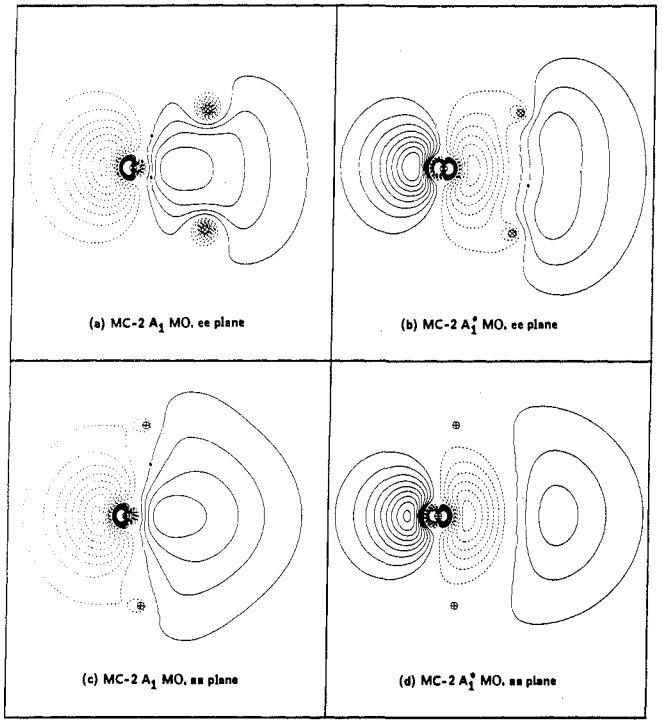

Figure 6. As Figure 2, and showing the two MC-2 orbitals in the Li_{eq}–Si–Li_{eq} and Li_{ax}–Si–Li_{ax} planes from the MC-2/3-21G(*) wave function.

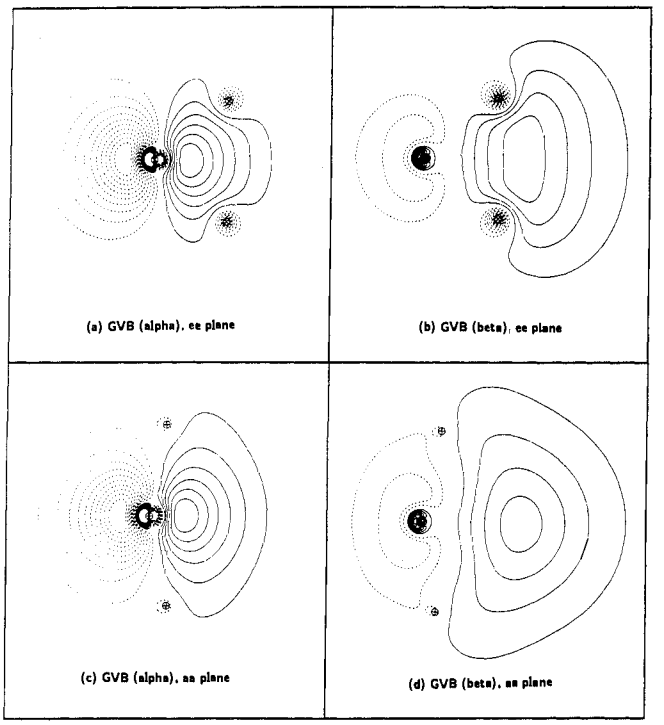

Figure 7. As Figure 2, and showing the two orbitals of the GVB pair in the Li_{eq}–Si–Li_{eq} and Li_{ax}–Si–Li_{ax} planes from the MC-2/3-21G(*) wave function.

orthogonality to the first orbital.

It is instructive to cast the MC-2 wave function into the equivalent one-pair generalized valence bond (GVB) form. The GVB pair functions are depicted in Figure 7; each of these is singly occupied, and they are coupled together as a singlet pair. In contrast to the MC-2 orbitals, the GVB pair orbitals both have a single node. The first GVB orbital (Figure 7a,c) is much more polarized toward silicon than is the first MC-2 orbital or the RHF HOMO, and the second GVB orbital (Figure 7b,d) is much more polarized toward the Li_{eq} atoms than is the second MC-2 orbital. The overlap between the two GVB orbitals is 0.55.

The contribution from Li_{ax} orbitals in the RHF LUMO, roughly equal to that from Li_{eq} orbitals (Figure 5b,d), is negligible in the MC-2 excited orbital, and the contributions from the Li_{eq} atoms are greatly increased (Figure 6b,d). This is consistent with the large decrease in the Li_{eq}–Li_{eq} distance compared to the Li_{ax}–Li_{eq} distances on going from RHF to MC-2 (0.20 vs 0.04 Å). There are four Li_{ax}–Li_{eq} interactions, but only one Li_{eq}–Li_{eq} interaction, and in an orbital constrained to maintain A_1 symmetry in the C_{2v} structure, the most favored interaction is Li_{eq}–Li_{eq}. Clearly, however, this represents a bias against Li_{ax}–Li_{eq} interactions. This bias could be essentially removed by including enough MCSCF configurations or, more easily, by including *all* double excitations in a second-order Møller–Plesset perturbation calculation (MP2). Our MP2/3-21G(*) optimizations confirm this suspicion of unbalance, as seen in Table I. Compared with MC-2, the Li_{eq}–Li_{eq} distance in the C_{2v} structure at the MP2 level decreased by only 0.01 Å, in contrast to the large decrease in the Li_{ax}–Li_{eq} distances of 0.09 Å. Just as in the RHF structure, the Li_{ax}–Li_{eq} distances are less than the Li_{eq}–Li_{eq} distance in the MP2 structure, the MP2 values being 3.17 and 3.22 Å, respectively. These distances are 0.12–0.15 Å less than the RHF/3-21G(*) values.

The relative energy of the C_{3v} structure with the 3-21G(*) basis set, which increased from 2.1 to 3.5 kcal/mol on going from RHF to MC-2, is reduced to 2.6 kcal/mol at the MP2 optimization level, showing that the MC-2 treatment selectively disfavors the C_{3v} structure with respect to the C_{2v} structure. The Li_{ax}–Li_{eq} distances in the C_{3v} structure decrease dramatically from 3.33 Å at RHF to 3.19 Å at MC-2 to 3.10 Å at MP2. As discussed at the beginning of this section, the $(A_1)^2 \rightarrow (A_1^*)^2$ configuration is unimportant in the T_d structure, with the consequence that it cannot be compared with the other structures at the MC-2 level. The relative energy of the T_d structure increases from 3.7 to 7.3 kcal/mol from RHF to MP2. The Li atoms in the T_d structure are much further apart than in the other structures (3.9 vs 3.1–3.2 Å), and the Li–Li bonding overlap within the virtual MOs is thus much weaker. The relative energy of the C_{4v} structure is nearly unaffected by the level of correlation treatment. Plots of the MP2 C_{2v}, C_{4v}, and C_{3v} structures are given in Figure 1.

To check on the reliability of the MP2 geometry optimizations, we also performed optimizations at the configuration interactions with full single and double excitation (CISD) level for the C_{2v} and C_{3v} structures. The maximum changes in Si–Li and Li–Li distances were found to be 0.016 and 0.012 Å, respectively. The C_{3v}–C_{2v} energy difference increased by only 0.05 kcal/mol. It is therefore probable that more comprehensive treatments of electron correlation would lead to similar geometries and relative energies. The total energies in Table I are higher with CISD than with MP2 because the former is variational and the latter is not.

Thus, Li–Li covalent bonding interactions in the C_{2v} structure of $SiLi_4$, already quite significant at the RHF-SCF level, increase significantly when the contribution of excited electron configurations to the wave function is included.

B. Influence of Basis Set. Having gained an understanding of the influence of correlation, we repeated the RHF and MP2 calculations with the larger 6-31G* basis set, as seen in Table I. Compared to the 3-21G(*) basis set, 6-31G* provides a much better representation of the core orbitals, as well as better valence orbitals (the addition of d orbitals on Li will have little effect, however). As a result, the 6-31G* total energies are more than 1.6 au lower than those of 3-21G(*), and basis set superposition errors, which could act to exaggerate the Li–Li bonding interactions, will be much reduced. Table I shows that the 6-31G* basis set decreases the Si–Li bond lengths and increases the Li–Si–Li bond angles. These changes are mild at the RHF level but are much more significant at MP2. For instance, the Li_{eq}–Si–Li_{eq} and Li_{eq}–Si–Li_{ax} angles in the C_{2v} structure are increased by 3° at MP2/6-31G* with respect to MP2/3-21G(*) and the Si–Li bonds contract by 0.05 Å. That is, the basis set errors are much more severe at the correlated level than at the SCF level, in accord with general experience. At the MP2/6-31G* level, the C_{3v} and C_{4v} structures are 2.9 and 4.0 kcal/mol, re-

Table II. Optimized Geometries and Energies of $GeLi_4$ and $SnLi_4$ Isomers[a]

sym	method	energy[b]	XA	XE	AE	EE	AXA	AXE	EXE
				$GeLi_4$ (X = Ge)					
C_{2v}	RHF	−2103.027 80 (0.00)	2.467	2.557	3.280	3.393	157.2	81.5	83.1
	MP2	−2103.200 82 (0.00)	2.474	2.533	3.220	3.285	153.7	80.0	80.8
C_{3v}	RHF	−2103.024 39 (2.14)	2.587	2.483	3.240	4.227		79.4	116.7
	MP2	−2103.196 75 (2.55)	2.545	2.484	3.140	4.196		77.3	115.3
C_{4v}	RHF	−2103.023 29 (2.84)	2.542	2.542	3.167	4.479	123.6	77.1	123.6
	MP2	−2103.194 93 (3.70)	2.538	2.538	3.117	4.408	120.5	75.8	120.5
T_d	RHF	−2103.020 18 (4.79)	2.438		3.982				
	MP2	−2103.189 67 (7.00)	2.435		3.977				
				$SnLi_4$ (X = Sn)					
C_{2v}	RHF	−6047.999 75 (0.00)	2.652	2.734	3.393	3.546	148.5	78.1	80.9
C_{3v}	RHF	−6047.996 99 (1.73)	2.755	2.680	3.366	4.514		76.5	114.7
C_{4v}	RHF	−6047.996 78 (1.86)	2.721	2.721	3.294	4.659	117.8	74.5	117.8
T_d	RHF	−6047.992 33 (4.65)	2.649		4.326				

[a] In the bond length and angle designations, the axial and equatorial lithium atoms are designated A and E, respectively. Distances in Å, angles in deg. [b] Total energy in au, and, in parentheses, relative energy in kcal/mol.

spectively, higher in energy than the C_{2v} minimum.

C. Triplet UHF Calculations. In our original paper,[1] a preliminary search of the triplet potential energy surface at the UHF level was carried out. The best structure was found to have D_{4h} symmetry but was 16.6 kcal/mol higher in energy than the C_{2v} RHF structure at the 3-21G(*) basis set level. This is a minimum at the UHF/3-21G(*) level and has a Si–Li bond length of 2.460 Å. At the UHF/6-31G* and UMP2/6-31G* levels [employing the 3-21G(*) geometries], the D_{4h} triplet is found to be 17.7 and 42.9 kcal/mol, respectively, higher in energy than the C_{2v} singlet. The two orbitals involving unpaired electrons in the D_{4h} triplet are the Si out-of-plane 3p(π) orbital, and a linear combination of the four Li 2p(π) orbitals of B_{2g} symmetry. However, an alternative triplet state, where the B_{2g} orbital is empty and a A_{1g} symmetry orbital composed from the four Li 2s orbitals is singly occupied, is lower in energy and prefers a distorted planar D_{2h} structure with Si–Li distances of 2.524 Å and Li–Si–Li angles of 75.5 and 104.5°. Both triplet states have significant spin contamination at the UHF/3-21G(*) level, with S^2 values of 2.11 and 2.26 for D_{4h} and D_{2h}, respectively. Optimization of a distorted tetrahedral structure of D_{2d} symmetry leads to the planar D_{4h} structure of the latter electronic state (with a singly occupied A_{1g} MO). The D_{2h} triplet is 2.69 kcal/mol lower in energy than the C_{2v} singlet at the UHF/3-21G(*) level. Upon UMP2/3-21G(*) optimization, however, the molecular symmetry of this state changes from D_{2h} to D_{4h} and the energy relative to the C_{2v} singlet increases to 19.36 kcal/mol. The existence of a low-lying triplet state for $SiLi_4$ thus seems unlikely.

Note that the lowest triplet states of $SiLi_4$ will involve (with respect to the singlet states) excitation from an orbital predominantly on Si to an orbital predominantly on the Li atoms. This is due to the ionic nature of $SiLi_4$. It is energetically most favorable to take the Si electron away from a pure p orbital, and this is at least part of the reason that the lowest energy triplet structures are planar. For $SiLi_4$, we were unable to find nonplanar triplet structures, in contrast to the case of CLi_4 (see Section VI).

V. $GeLi_4$ and $SnLi_4$ Structures

The results of our RHF geometry optimizations of $GeLi_4$ and $SnLi_4$, presented in Table II, are quite similar to those of $SiLi_4$. Analytic vibrational frequency calculations verify that the C_{2v} structures of $GeLi_4$ and $SnLi_4$ are energy minima. In the case of $GeLi_4$, MP2 optimizations also were performed (Table II). While the T_d structures have higher RHF relative energies than in $SiLi_4$ (4.6–4.8 vs 3.7 kcal/mol, respectively), the C_{4v} structures have a much lower relative energy, so that the RHF energy span between the C_{2v}, C_{3v}, and C_{4v} structures decreases from 3.7 (Si) to 2.8 (Ge) to 1.9 kcal/mol (Sn). The relative energies for all four structures of $SiLi_4$ and $GeLi_4$ are quite similar at the MP2 level, however, and this serves as warning against overinterpreting the RHF results. As is reflected in the small calculated difference in bond lengths in T_d $SiLi_4$ and $GeLi_4$ (0.02 Å), the covalent radius of Ge is only 0.04 Å larger than that of Si. Since the Li–X–Li bond angles decrease by 1–5° on going from X = Si to X = Ge, the Li–Li distances are in certain cases even smaller in $GeLi_4$ than in $SiLi_4$ at the RHF level (i.e., the Li_{ax}–Li_{eq} distances in the C_{3v} and C_{2v} isomers). Reoptimization of the $GeLi_4$ structures at the MP2 level (Table II) results in Li–Li distances that are in all cases longer than the corresponding $SiLi_4$ values, however. The MP2 Li–X–Li bond angles are about the same or slightly greater in $GeLi_4$ as in $SiLi_4$. The covalent radius of Sn is about 0.22 Å greater than that of Si, and the Li–Li distances in $SnLi_4$ are significantly larger than in $SiLi_4$ (see Table II).

Table III. Optimized Geometries[a] (RHF Level for Singlets, UHF Level for Triplets) and Relative Energies[b] (kcal/mol) of CLi_4 Species

sym	basis	R	θ	α	HF[c]	MP2	MP4
			Singlets				
T_d	3-21G	1.929			0.00 (0)		
	6-31G*	1.909			0.00 (0)	0.00	0.00
C_{4v}	3-21G	2.050	85.8	74.3	13.04 (1)		
D_{4h}	3-21G	1.982	90.0		14.36 (2)		
			Triplets				
D_{2d}	3-21G	2.018	97.3	69.0	−11.60 (0)		
	6-31G*	2.020	96.3	70.6	−13.18	38.38	35.32
D_{2h}	3-21G	2.066	83.5		−10.99 (0)		
	6-31G*	2.057	82.7		−13.97	47.15	44.02

[a] R (in Å) is the C–Li distance, θ (in deg) is the smallest Li–C–Li angle, and α (in deg) is the angle between the C–Li bonds and the major symmetry axis of the molecule. [b] MP2 and MP4 (MP4SDTQ) energies are given at the HF geometries. Total energies can be derived from those for the T_d singlet species (in au): −67.13154 (3-21G), −67.51957 (6-31G*), −67.75018 (MP2/6-31G*), −67.77356 (MP4/6-31G*). [c] The analytically determined total number of imaginary vibrational frequencies of the optimized structure is given in parentheses.

VI. Reinvestigation of CLi_4

This work stimulated us to reinvestigate CLi_4[2] to determine whether the tetrahedral singlet is the lowest energy structure. Since planar and tetrahedral (and singlet and triplet) forms of H_2CLi_2 are close in energy,[6] the same might possibly be true for CLi_4. Our results are given in Table III. Through analytic vibrational frequency calculations, we found the T_d singlet of CLi_4 to be an energy minimum at both the HF/3-21G and HF/6-31G* levels. Alternative singlet structures of C_{4v} and D_{4h} symmetry were found to be 13.0 and 14.4 kcal/mol higher in energy, respectively, at the HF/3-21G level, and neither of these structures are minima. Triplet structures of nonplanar D_{2d} and planar D_{2h} symmetry (both energy minima) are found to be 13–14 kcal/mol lower than the T_d singlet at UHF/6-31G*, however. These are heavily spin contaminated, with S^2 values of 2.56 and 2.68, respectively. As seen from Table III, these triplet structures are more than 35 kcal/mol *higher* in energy than the T_d singlet when electron correlation is included at the MP2 and MP4 levels. In addition, a distorted nonplanar triplet structure of C_2 symmetry was discovered that is 7.8 kcal/mol lower in energy than D_{2d} at UHF/3-21G. It has significantly greater spin contamination than the D_{2d} triplet (S^2 = 2.92) and is even higher in energy than D_{2d}

when electron correlation is included. We thus find that the only energetically reasonable form for CLi_4 to be the T_d singlet, in contrast to the case of $SiLi_4$, where the T_d structure exhibits three imaginary vibrational frequencies.[1]

VII. Conclusion

We find C_{2v} structures with unusually small Li-X-Li bond angles to be favored for $SiLi_4$, $GeLi_4$, and $SnLi_4$. Delocalization from the $\sigma(X-Li_{eq})$ and $\sigma(Li_{ax}-X-Li_{ax})$ bonding orbitals into the low-occupancy 2s and 2p orbitals of the other lithium atoms results in effective Li-Li attractive interaction at the RHF level, as illustrated by our orbital plots. The importance of the lithium 2p orbitals in acting as acceptors in such interactions is illustrated by our finding that $SiLi_4$ would be tetrahedral in the absence of Li 2p orbitals. By contrast, the only important structure for CLi_4 is found to be the T_d singlet.

For $SiLi_4$, inclusion of electron correlation effects favor even smaller Li-Si-Li bond angles and destabilize the T_d structure with respect to the C_{2v} structure further. The essence of this correlation effect is described at the two-configuration MCSCF (MC-2) level and involves excitation of $(A_1)^2 \rightarrow (A_1^*)^2$ type. The MC-2 description is unbalanced with respect to Li-Li bonding, however, as the excited configurations contributing most strongly to the four $Li_{eq}-Li_{ax}$ bonding interactions are omitted. A more balanced treatment of correlation effects is given at the full double excitation MP2 level. More refined treatment of correlation at the full CISD level yields results nearly identical with those of MP2, showing that the simple MP2 perturbational treatment provides a good approximation of the CISD variational result. These correlation effects on molecular geometry are smaller when the 6-31G* basis set is employed instead of 3-21G(*). Similar results are found at the MP2 level for $GeLi_4$.

Acknowledgment. This work was supported by the Deutsche Forschungsgemeinschaft, the Fonds der chemischen Industrie, the Volkswagen Stiftung, and Convex Computer Corp. We thank Prof. R. W. F. Bader and Prof. R. J. Lagow for stimulating correspondence and Prof. E. Heilbronner for his interest.

Registry No. Li_4Si, 63784-76-9.

Interaction of Calcium and Magnesium Ions with Malonate and the Role of the Waters of Hydration: A Quantum Mechanical Study

David W. Deerfield, II,*,† Douglas J. Fox,† Martin Head-Gordon,‡ Richard G. Hiskey,§ and Lee G. Pedersen§,∥

Contribution from The Pittsburgh Supercomputing Center, 4400 Fifth Avenue, Pittsburgh, Pennsylvania 15213, AT&T Bell Laboratories, Murray Hill, New Jersey 07974, the Department of Chemistry, CB 3290, The University of North Carolina at Chapel Hill, Chapel Hill, North Carolina 27599-3290, and NIEHS, Research Triangle Park, North Carolina 27709. *Received March 21, 1990*

Abstract: The structure of malonate interacting with either a Ca(II) or a Mg(II) ion in a chelation bidentate orientation has been studied with ab initio molecular orbital theory. In addition, the optimized chelation bidentate structures have also been determined for the enol tautomer of malonate ion and two different deprotonated forms of the malonate–metal ion complex. All malonate-derived structures were optimized with and without four waters of hydration about the divalent metal ion. The enol tautomer of malonate was found to be less stable than the keto form complexed with either Ca(II) or Mg(II) ions. Computations have demonstrated that removal of a proton from one of the waters of hydration about the divalent metal ion leads to a structure that is calculated to be more stable than the structure resulting from the deprotonation on carbon of the malonate complex. A mechanism for the chemical modification and proton exchange of proteins containing γ-carboxyglutamic acid (e.g., prothrombin), for which malonic acid serves as a model, is proposed.

Introduction

γ-Carboxyglutamic acid (Gla) is formed in a posttranslational, vitamin K mediated carboxylation of specific glutamyl residues.[1] The net result of this modification is the conversion of the substituted acetic acid side chain of Glu into the substituted malonic acid of Gla. It is the malonic acid functionally that is responsible for the ability of coagulation zymogens to bind divalent metal ions [usually Ca(II) or Mg(II)] under physiological conditions.[2,3] For the vitamin K dependent coagulation proteins [e.g., factors II (prothrombin), VII, IX (Christmas), and X (Stewart) and proteins C, S, and Z], the binding of divalent metal ions is required prior to physiological activity (either formation of binary or ternary protein complexes or the assembly of an active enzyme and co-enzyme embedded on an acidic phospholipid surface interacting with substrate). Ca(II) ions, but not Mg(II) ions, will support the coagulation cascade at significant rates under physiological conditions.[2,3] Furthermore, low concentrations of Mg(II) ions in the presence of Ca(II) ions will exert a synergistic influence on the rate of clot formation.[2] Thus, one of the basic questions of the coagulation protein literature deals with differentiating the roles of these two divalent metal ions. Specifically, are the interactions of Ca(II) and Mg(II) ions with the malonate side chain of Gla similar? Or does the observed metal ion specificity reside in a different portion of the coagulation process (e.g., in the binding of metal ions to either the acidic phospholipid surface or the glycosylated part of the protein)?

*Author to whom correspondence should be addressed.
†The Pittsburgh Supercomputing Center.
‡AT&T Bell Laboratories.
§The University of Nort Carolina.
∥NIEHS.

(1) Suttie, J. W.; Jackson, C. M. *Physiol. Rev.* **1977**, *57*, 1-70. Suttie, J. W. *CRC Crit. Rev. Biochem.* **1980**, *8*, 191.
(2) Bloom, J. W.; Mann, K. G. *Biochemistry* **1978**, *17*, 4430-4438.
(3) Deerfield, D. W., II; Olsen, D. L.; Berkowitz, P.; Byrd, P.; Koehler, K. A.; Pedersen, L. G.; Hiskey, R. G. *J. Biol. Chem.* **1987**, *262*, 4017-4023.

0002-7863/91/1513-1892$02.50/0